



RESEARCH ARTICLE

Mortality versus survival in drought-affected Aleppo pine forest depends on the extent of rock cover and soil stoniness

Yakir Preisler^{1,2}  | Fyodor Tatarinov¹ | José M. Grünzweig² | Didier Bert³ | Jérôme Ogée⁴ | Lisa Wingate⁴ | Eyal Rotenberg¹ | Shani Rohatyn^{1,2} | Nir Her⁵ | Itzhak Moshe⁵ | Tamir Klein⁶  | Dan Yakir¹

¹Earth and Planetary Science Department, Weizmann Institute of Science, Rehovot, Israel; ²Robert H. Smith Faculty of Agriculture, Food and Environment, The Hebrew University of Jerusalem, Rehovot, Israel; ³BIOGECO, INRA, University of Bordeaux, Cestas, France; ⁴ISPA, Bordeaux Science Agro, INRA, Villenave d'Ornon, France; ⁵Forestry Department, KKL, Gilat, Israel and ⁶Plant & Environmental Sciences Department, Weizmann Institute of Science, Rehovot, Israel

Correspondence

Dan Yakir

Email: dan.yakir@weizmann.ac.il

Funding information

KKL research Fund, Grant/Award Number: 90-10-012-11; Ministry of Science & Technology, Israel & ministry of Foreign affairs and international development (MAEDI), and Ministry of National Education and Research (MENESER) of France, Grant/Award Number: 3-6735

Handling Editor: Anna Sala

Abstract

1. Drought-related tree mortality had become a widespread phenomenon in forests around the globe. This process leading to these events and its complexity is not fully understood. Trees in the dry timberline are exposed to ongoing drought, and the available water for transpiration in the soil can determine their survival chances.
2. Recent drought years led to 5%–10% mortality in the semi-arid pine forest of Yatir (Israel). The distribution of dead trees was, however, highly heterogeneous with parts of the forest showing >80% dead trees (D plots) and others with mostly live trees (L plots). At the tree level, visible stress was associated with low pre-dawn leaf water potential at the dry season (−2.8 MPa vs. −2.3 MPa in non-stressed trees), shorter needles (5.5 vs. 7.7 mm) and lower chlorophyll content (0.6 vs. 1 mg/g dw). Trends in tree-ring widths reflected differences in stress intensity (30% narrower rings in stressed compared with unstressed trees), which could be identified 15–20 years prior to mortality.
3. At the plot scale, no differences in topography, soil type, tree age or stand density could explain the mortality difference between the D and L plots. It could only be explained by the higher surface rock cover and in stoniness across the soil profile in the L plots. Simple bucket model simulations using the site's long-term hydrological data supported the idea that these differences could result in higher soil water concentration (m^3/m^3) in the L plots and extend the time above wilting point by several months across the long dry season.
4. Accounting for subsurface heterogeneity may therefore critical to assessing stand-level response to drought and projecting tree survival, and can be used in management strategies in regions undergoing drying climate trends.

KEYWORDS

semi-arid, soil moisture, stoniness, surface rock cover, tree rings, Yatir Forest

1 | INTRODUCTION

Trends in climate change implicating decreased rainfall amounts and increased drought intensity (Gao & Giorgi, 2008; IPCC [Intergovernmental Panel on Climate Change], 2013) lead to episodes of forest decline globally (Allen et al., 2010; Breshears et al., 2009). This decline is often associated with secondary stress factors, such as insect damage (McDowell, 2011), reduced growth and development of mature trees (Suarez, Ghermandi, & Kitzberger, 2004) and drought legacy damage (Anderegg et al., 2013; Peltier, Fell, & Ogle, 2016), often expressed by early decline in tree-ring width (RW) prior to mortality (Cailleret et al., 2017; Colangelo et al., 2017), and ultimately influencing large-scale water and carbon cycling (Allen et al., 2010; Anderegg et al., 2012).

Processes underlying mortality at the tree scale have been extensively studied in recent years, addressing the physiological mechanism of tree mortality (Dickman, McDowell, Sevanto, Pangle, & Pockman, 2015; McDowell et al., 2008; Parolari, Katul, & Porporato, 2014). However, at the stand and at the ecosystem scales the causes leading to mortality are less established, ranging from the site slope and aspect (mostly south-facing, high radiation), elevation and tree density (both positive or negative effect; Huang & Anderegg, 2012; Soulé & Knapp, 2007; Worrall et al., 2008) to soil parent material and soil texture (Gitlin et al., 2006; Koepke, Kolb, & Adams, 2010). In dry regions, the transpirable amount of soil water can be significantly lower than total precipitation input (Klein et al., 2012; Ritchie, 1981), and clearly, low soil water retention capacity negatively affects tree survival (Peterman, Waring, Seager, & Pollock, 2013). Drought impact on trees is also expressed by changing the root:shoot ratio, the size of the existing root system and its ability to extract water (Klein, Cohen, & Yakir, 2011; Padilla, Miranda, & Pugnaire, 2007). The actual soil water availability is affected by the local meteorological conditions (Precipitation, VPD, etc.) and by habitat characteristics. Among these characteristics are soil depth and stoniness fraction, rock cover and rooting depth. Shallow and rocky soils were traditionally considered poor habitats for tree development, allegedly because of the inherent lack of resources (Oppenheimer, 1957; Suarez et al., 2004). However, rock fragments at the surface and in the soil profile can have variable effects on soil moisture content, soil evaporation and soil water availability, which can alter the water availability in the soil and can also be in favour for desert plants as suggested by Poesen and Lavee (1994). The rooting depth is coupled with these habitat characteristics and with soil moisture, resulting in a feedback process which eventually results in changes in soil water content (SWC) and water uptake by the roots to transpiration.

The Mediterranean region is projected to experience climatic warming and drying trends during this century (Alpert, Krichak, Shafir, Haim, & Osetinsky, 2008; Gao & Giorgi, 2008), and consequently, enhanced drought-related dieback of tree species not adapted to extreme conditions is expected. Aleppo pine (*Pinus halepensis*), one

of the major tree species in this region (Schiller & Atzmon, 2009), is showing adjustments to extreme drought conditions, for example by shifting leaf gas exchange seasonally to early spring, and to early morning hours in order to reduce water loss (Maseyk et al., 2008). Despite these adjustments, increased drought-related mortality was observed in these Aleppo pine populations during the past decade (Dorman, Perevolotsky, Sarris, & Svoray, 2015); however, the specific tree and plot-scale factors leading to these mortality events are still unclear.

The Yatir Forest, planted in the mid-1960s at the “dry timberline” with mean annual precipitation of 280 mm, experienced six extreme drought years between 1996 and 2013, four of which were consecutive events of two drought years each (Figure 1, Supporting Information Figure S1). By September 2011, an unprecedentedly high mortality rate of 5%–10% was documented across the forest indicating a limit to the forest drought resistance. However, even under these extreme conditions, a striking spatial mortality pattern indicated that tree die-off occurred in patches, with significant areas across the forest showing no mortality and only mild stress effects.

The objective of this study was to identify the geophysical and ecophysiological factors associated with tree drought stress that can explain the distinct patchiness of tree mortality within the forest tree matrix.

2 | MATERIALS AND METHODS

2.1 | Research area

The study was conducted in the Yatir Forest (31°20'N 35°03'E, 550–700 m a.s.l.), a 50-year-old forest planted predominantly with Aleppo pine (*P. halepensis* Mill.) trees. Minimum and maximum daily mean temperatures during the coldest and the warmest months are $2.5 \pm 0.7^\circ\text{C}$, $21.2 \pm 1.2^\circ\text{C}$, $16.1 \pm 0.5^\circ\text{C}$ and $35.1 \pm 0.9^\circ\text{C}$, respectively. Mean annual precipitation (P) is 280 ± 80 mm (1965–2013), potential evapotranspiration (PET) is 1,600 (mm/year), and P/PET is 0.17. Soil type was classified as light Rendzina (Haploxeroll) above porous chalk and limestone, with a deep, inaccessible, groundwater table (>300 m depth; GrünzweigGelfand, Fried, & Yakir, 2007). The annual-scale hydrological budget in this site was shown to be nearly balanced, with evapotranspiration (ET) = $0.94P$ (where ET and P are annual-scale evapotranspiration and precipitation; Yaseef, Yakir, Rotenberg, Schiller, & Cohen, 2009). The hydrological years 2007–2008 and 2008–2009 were two extreme drought years, with an unusually long dry season of with 349 days without a rain event of >5 mm (Figure 1a; rain amounts ≤ 5 mm in spring and autumn are considered immediately lost to evaporation).

2.2 | Study sites

The research design consisted of 20 study sites, with each site containing one plot in which >80% of the trees died (D plots), and an

adjacent plot with >80% live trees as of May 2011 (L plots; a total of 40 plots of 800 m²; Supporting Information Figure S2). Mortality patterns were first identified from aerial photography of the Forestry Services, and study plots were arbitrarily selected across the forest, and subsequently accessed on the ground, avoiding only plots inaccessible with trenching equipment (see Supporting Information Figure S2). Each plot was studied by means of ground-based inventory of tree characteristics (diameter at breast height [DBH], height, age and density); physiographical survey (slope, aspect and elevation); soil properties (detailed below); bark beetle presence (evidence of galleries and emergence holes); and a dendrochronology study (detailed below).

The above-ground biomass was determined at all 20 sites by measuring tree height and DBH, and applying site-specific allometric equations (Grünzweig et al., 2007). The biomass of a few cut trees logged in the framework of this study was determined by calculating DBH from measured basal diameter.

In five representative out of the 20 sites, the L plots were selected for more intensive measurements. In these plots, trees were classified into three stages of stress: healthy (S-0), stressed (S-1) and dying (S-2). Healthy trees had a dense canopy of long, green needles, while stressed trees typically had a sparse canopy of short, yellowish needles. Dying trees had only brown and no green leaves. At the five selected plots, two trees from each of the

three stress categories were selected for detailed measurements ($n = 10$ trees per category).

2.3 | Tree-ring analysis

The history of tree-growth dynamics was analysed in the three stress categories from the five selected L plots using dendrochronology. During May–August 2011, two cores were extracted at breast height by a 20-cm increment borer (core diameter 5.15 mm) equipped with a starter (Haglof, Sweden) at opposite sides of the trunk, at 0° (N) and 180° (S) from S-0 and S-1 trees. Five to six cores were taken from each of the 5 L plots ($n = 54$ cores), and 14 cores were taken from dying/dead trees, complemented with 17 complete discs of dead trees ($n = 31$ cores and discs). All cores and discs were scanned (1,600 dpi, Epson, USA) after proper sanding, and the images were analysed with WinDENDRO software (Regent Instruments Inc., Canada). Tree rings were cross-dated with the site precipitation records ($R^2 \geq 0.80$) using the “Gleichläufigkeit” agreement test based on Eckstein and Bauch (1969) and Schweingruber, Bartholin, Schaur, and Briffa (1988). Annual precipitation also helped in the detection of missing rings in extremely dry years. Basal area increment (BAI) was calculated from the measured annual RW at the two sides of each tree (cores or discs) using a simple area calculation of the cumulative radius of each year $\frac{(r^2)}{100}$, where r is the cumulative

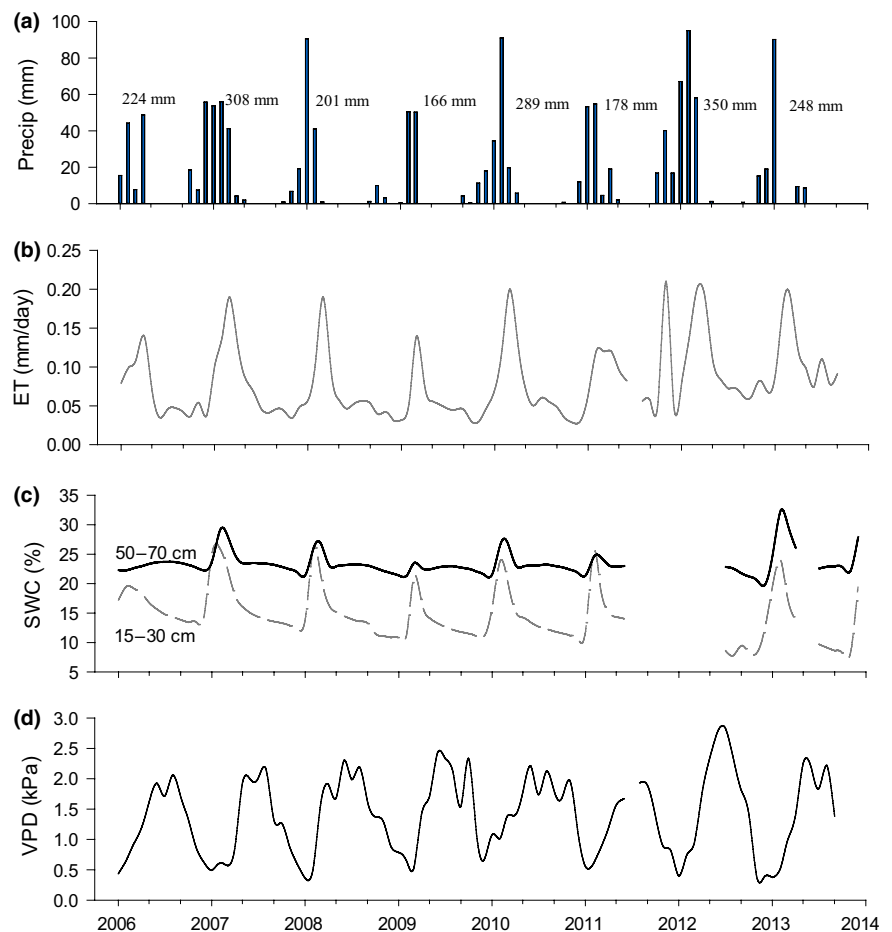


FIGURE 1 Climatic record in Yatir Forest for the period of 2006–2014 (mean monthly records). (a) Precipitation; (b) evapotranspiration (ET); (c) volumetric soil water content, (SWC); (d) vapour pressure deficit (VPD). For each year, the annual total precipitation is shown at the right side of the precipitation bars (a). Missing data in SWC (c) are due to sensor failure during that period. All data were obtained from the nearby flux tower measurements

RW up to the current year). Single missing years identified using the climatic cross-dating were considered as having an annual RW = 0.

2.4 | Tree water potential and needle properties

Detailed growth and physiological measurements were also carried out in five L plots. Seasonal measurements of pre-dawn leaf water potential (WP) (ψ_{pd}) were conducted on the healthy and stressed trees every 3 months between August 2012 and August 2013, using the pressure chamber technique (PMS Instrument Company, OR, USA). Live needles of 3–4 cohorts (1 cohort per year) were also collected from the healthy and stressed trees in each of the intensive study plots in October 2012, at the end of the needle elongation period (Maseyk et al., 2008) for needle measurements. Needle length of the three cohorts was measured on 10 needles per cohort with a ruler. For chlorophyll analysis, 1-year-old needles were used. Concentrations of chlorophylls *a* and *b* were determined following the subtraction of the absorbance of a blank sample according to Porra (2002). The 1- to 3-year-old needles were also analysed for nitrogen concentration of S-0 and S-1 trees after leaves were oven-dried at 60°C for 48 hr and ball-milled. The concentration of total needle nitrogen was determined using an elemental analyser (Thermo, EA 1108, Meersburg, Germany) and was expressed on a dry weight basis. More details are available at the Supporting Information Appendix S1.

2.5 | Soil properties and root distribution along soil profiles

The assessment of soil and root characteristics along the soil profile was conducted in 11 out of the 20 study sites (total of 22 paired plots). Soil trenches 7 ± 1.6 m long and 1.5 ± 0.6 m deep (mean \pm SE; with a maximum depth of 2 m or less if bedrock depth was shallower) were dug at a random location, in places without a rocky surface that prevented digging, around the centre of each of the L and D plots at the 11 sites. Each trench was divided into three equal sampling sections across the entire length of the trench. Each section was analysed from the soil surface to the maximum depth of each trench. In each of the three sampling sections per trench, root distribution and stoniness were estimated visually using a 20 cm \times 20 cm frame. Coarse roots (diameter > 2 mm) were counted in situ in each frame to assess root density. Root diameters were measured using a digital calliper (Fuji, Japan; ± 0.03 mm deflection). Likewise, stoniness was visually estimated as the fraction of stones (Supporting Information Figure S3). Stones considered in this survey were between 2 and 75 mm in diameter, consistent with the definition of “gravel” (see Poesen & Lavee, 1994). Stoniness was reported to a maximal depth of 1.2 m, with the soil depth determined as the vertical distance from the soil surface. In addition, the area of surface rock cover was assessed in a survey consisting of 36 sampling points in each plot (Supporting Information Figure S4) for the entire surface area using a metal rod to determine near surface rock presence. Surface rock included stones larger than ~100 mm that were embedded in the soil.

2.6 | Quantifying stoniness effects on soil water content

To obtain a preliminary quantification of the potential effects of stoniness, surface rock cover, water storage in stones and differences in tree size on SWC, simulations were carried out using a simple 1D “bucket model.” Briefly, we solved for changes in SWC over time in a given soil depth using Equation (1), with the left term providing the output discussed in the results below. The main terms of the bucket model were based on input data from the site, including variations in rock cover and stoniness, and with root uptake and transpiration were constrained by sap flux data from the flux tower, L plot. Precipitation, air temperature, VPD, evapotranspiration and sap flow measured in 2011 were obtained from the continuously operating flux tower L plot and were used as model input, with SWC data used for tuning and validation. The main goal of the modelling exercise was to test our hypothesis that the effects of rock cover and stoniness underlie the observed differences between the L and D plots. The model was adopted from earlier versions (Hlaváčiková, Novák, & Šimůnek, 2016; Novák, Křáva, & Šimůnek, 2011) using the extensive data of the long-term Yatir site (e.g., Tatarinov et al., 2016) and was based on simple diffusion equations (e.g., Slayter, 1967), adjusted to our specific site conditions:

$$\frac{\partial \text{SWC}(z,t)}{\partial t} = -\frac{\partial q(z,t)}{\partial z} - R(z,t) - f(z,t) \quad (1)$$

where $q(z,t)$ is vertical soil water flux, $R(z,t)$ is root uptake, $f(z,t)$ is flux between soil and stones (positive when going from soil to stones), and $W(z,t)$ is stone water content (for more details, see Supporting Information Appendix S1). Note that we used SWC, and not WP, using the specific soil moisture retention curve for Yatir soil to avoid WP values towards infinity when soils dry. In wetter conditions, no differences between simulations using WP or SWC were observed. The transpirable SWC threshold ($t\text{SWC} = 0$) used to assess the simulation results was based on Klein et al. (2012) as $\text{SWC} = 16.1\%$ in the 10–60 cm soil layer. The chalky stones storage capacity of 1%–7% by volume was estimated in soaking and drying experiments in the laboratory using random stone samples from both plots.

2.7 | Statistical analysis

Geophysical, stand and tree characteristics were analysed for significant differences between L and D plots by a paired *t* test. Tree-ring and physiological variables were analysed for differences among the tree categories (two or three levels) by a one-way analysis of variance (ANOVA). Multiple comparisons were performed using Tukey–Kramer HSD test, adjusted by the Holm–Šidák correction where necessary. Statistical analyses were performed by SigmaPlot 12 (SYSTAT Software, Erkrath, Germany) and JMP7 software (SAS Institute, Cary, NC, USA).

TABLE 1 Tree and needle characteristics in healthy, stressed and dead trees

Tree category	Height (m)	DBH (cm)	1-year-old Needle length (cm)	Nitrogen content (%)	Chlorophyll content (mg/g)	Bark beetle presence (%)
Healthy (S-0) (in 2011–2012)	11.2 (0.6) ^b	22.1 (1.5) ^b	7.7 (0.05) ^a	1.03 (0.05) ^a	1.00 (0.03) ^b	0 (0) ^c
Stressed (S-1) (in 2011–2012)	8.3 (0.9) ^a	15.5 (2.6) ^a	5.5 (0.01) ^b	1.01 (0.02) ^a	0.60 (0.05) ^a	40 (5) ^b
Dead (S-2) (in 2010)	7.9 (0.6) ^a	15.0 (2.8) ^a	–	–	–	100 (0) ^a

Note. Means, with standard errors in brackets. Trees were sampled in 5 L (live) plots, all of which had a small fraction of dead trees (<20%), $n = 5$ trees in a category at each plot. Different letters indicate statistically significant differences among tree categories at $p < 0.05$ (Tukey–Kramer HSD test).

3 | RESULTS

We examined possible explanations for the observed mortality and its spatial heterogeneity along the following two main lines: first, at the tree scale, both by comparing trees in the L (live) and D (dead) plots based on above-ground and below-ground parameters, and by comparing trees in three pre-defined stress levels in L plots; second, at the plot scale, based on a survey of L and D plots and based on extensive soil trenching to examine the sub-surface conditions.

3.1 | Tree-scale drought responses

The S-0 (healthy) trees were larger (in height and DBH) than both the S-1 (stressed) and S-2 (dying) trees, with the two latter categories being similar in size (Table 1). Chlorophyll concentration in 1-year-old needles was considerably higher, but nitrogen concentration in 1- to 3-year-old needles was similar in the S-0 compared to the S-1 trees. The needles of the S-0 trees were significantly longer by 1.7 ± 0.3 cm across three cohorts than the needles from the S-1 trees. Evidence of bark beetles presence was noted in all S-2 trees and in 40% of S-1 trees, while S-0 trees had no bark beetle at all (Table 1). However, the relationship between needle length and precipitation was not markedly different between tree classes ($p > 0.05$; Supporting Information Figure S5).

Comparing living trees of the two categories in the five representative L plots in August 2012 indicated significantly higher mean pre-dawn WP (ψ_{pd}) in the S-0 than the S-1 trees (Figure 2). The first small rain event in November 2012 did not alleviate the drought stress and did not improve the ψ_{pd} values of the trees, but actually narrowed the difference between the categories due to a decrease in ψ_{pd} of S-0 trees. By the end of the rainy season in February 2013, ψ_{pd} had increased considerably, eliminating the differences between tree categories. The differences widened again in the next dry season (May and August 2013), with ψ_{pd} in the S-1 reaching values lower by 0.7 MPa compared with the values in the previous summer (-3.2 vs. -2.5 MPa).

Tree-ring dynamics in the selected trees of the different stress levels indicated a divergence in the BAI trends between the live (both S-0 and S-1) and the dead trees (Figure 3). This

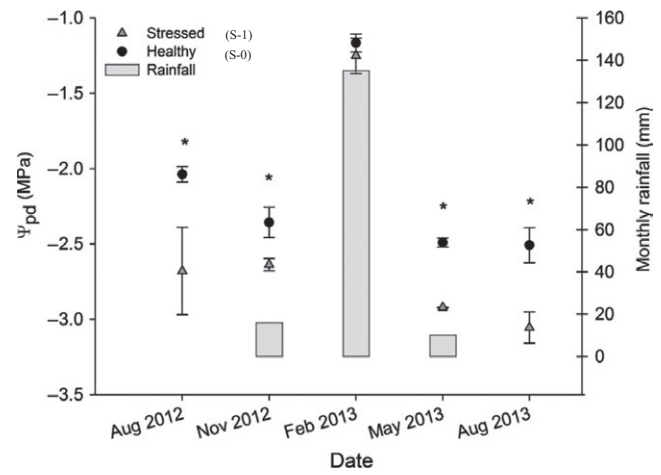


FIGURE 2 Seasonal variation of pre-dawn water potential in healthy versus stressed trees ($n = 5$ plots for each tree category). Asterisks indicate statistically significant differences among tree categories at $p < 0.05$ (Tukey–Kramer HSD test). Monthly precipitation is shown in the gray bars.

divergence started following the signature drought of 1984 ($p = 146$ mm) followed by two dry years. Between 1984 and 2010, the BAI of the healthy trees was higher by $152 \pm 16\%$ on average than the BAI of the trees that died in the 2010 mortality event. It seems that 2005 indicated the onset of the final decay leading to this event, 5 years prior to actual mortality. Another divergence in the BAI trend was observed between S-0 and S-1 trees starting in 1996, apparently in response to the 1995–1996 dry years. From that period on, S-0 trees had $176 \pm 12\%$ higher BAI than S-1 trees. The radial growth of all trees showed a strong and significant link to water availability, as expressed in the correlation coefficient and p values of the BAI and annual precipitation. For the period of 1977–2012, the correlation coefficient was 0.632 ($p < 0.005$), 0.592 ($p < 0.005$) and 0.464 ($p = 0.005$) for the S-0, S-1 and S-2 trees, respectively.

3.2 | Plot-scale drought responses

At the plot level, DBH, basal area, height and above-ground biomass were all significantly larger in the L compared with the D

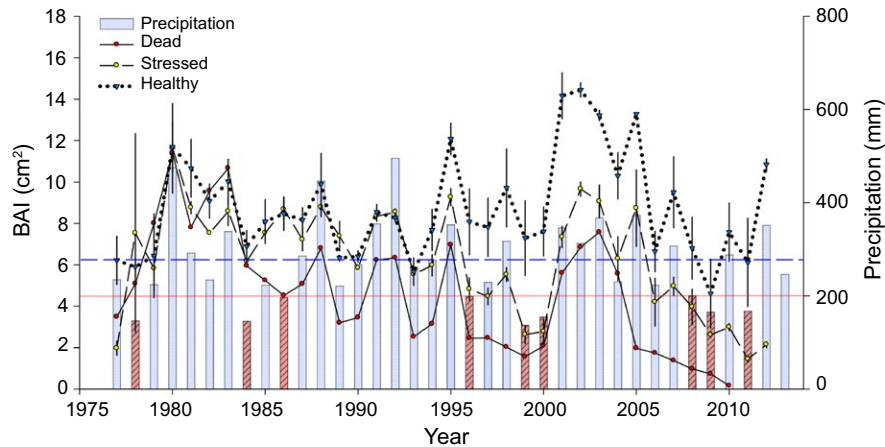


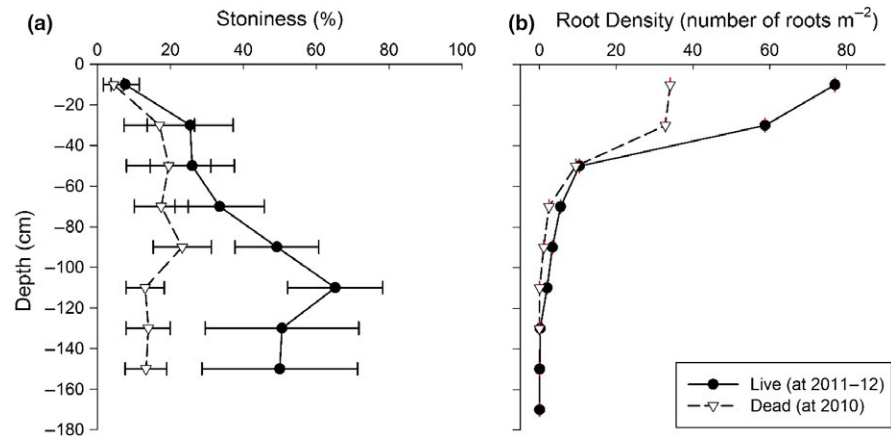
FIGURE 3 Comparison of annual basal area increment (BAI) among healthy, stressed and dead trees ("dead" trees died in 2009–2010) sampled at the five intensively studied sites. Bars show annual precipitation. The dashed blue line represents mean annual precipitation (280 ± 80 mm), and the full red line indicates the 200 mm line defined as the drought threshold. Red dashed precipitation bars represent drought year with annual rainfall below 200 mm

TABLE 2 A comparison between live (L) (at 2011–2012) and dead (D) (in 2010) plots and their main descriptive characteristics

Characteristics	No. of sites	L plots	D plots	p Value
<i>Tree characteristics</i>				
Tree diameter (cm)	20	17.5 (0.7)	15.0 (0.6)	0.023
Tree basal area (cm ²)	20	133.2 (2.8)	102 (2.5)	0.031
Tree height (m)	20	10.25 (0.5)	8.8 (0.3)	0.011
Tree AG biomass (kg/tree)	20	134.5 (17)	79.1 (8)	0.014
<i>Stand characteristics</i>				
Stand basal area (m ² /ha)	20	4.74 (0.4)	3.7 (0.3)	0.013
Above-ground biomass (kg/plot)	20	4,552 (613)	2,925 (305)	0.011
Planting density (trees/ha)	20	600 (47)	615 (51)	0.846
Current tree density (trees/ha)	20	356 (26)	364 (31)	0.917
Tree age (year)	20	42.3 (2.2)	42.3 (2.4)	0.541
<i>Geophysical characteristics</i>				
Elevation (m a.s.l.)	20	646 (9)	645 (8)	0.452
Slope (°)	20	6.7 (1)	6.8 (1)	0.476
Aspect (°)	20	245 (19)	254 (24)	0.382
<i>Root characteristics</i>				
Root cross sectional area (cm ²)	11	1,683 (365)	917 (221)	0.044
Root density (# of roots/m ²)	11	755.7 (11.4)	615.9 (10.3)	0.354
Root:shoot index	11	20.3 (5.7)	14.1 (4.4)	0.199
<i>Soil characteristics</i>				
Soil depth	11	74 (11.5)	102 (11.7)	0.053
<i>Stoniness (%)</i>				
0–1.2 m	11	48 (4.9)	15 (3.1)	<0.001
0–0.6 m	11	23.1 (5)	14.6 (4.2)	0.101
0.6–1.2 m	11	60.1 (6.7)	21.3 (4.6)	<0.001
Surface rock cover (%)	11	36.8 (7)	8.8 (3)	0.004

Note. The L plot at each site had >80% live trees, the D plot had >80% dead trees; in each plot, all live and dead trees were measured. Root cross-sectional area was measured at the top 60 cm of the soil profile. Above-ground biomass was calculated using specific allometric equations. Soil depth, stoniness fraction and surface rock cover as obtained from the trenches excavated in 11 sites. Soil cover was determined by the rock/soil presence in the surface. Stoniness was averaged every 20 cm across the top 1.5 m of the soil profile. Values are means, with standard errors in brackets. *p* Values are probabilities from paired *t* tests; statistically significant differences ($p \leq 0.05$) are indicated in bold. Planting density was calculated as the sum of tree and stumps (singular) densities.

FIGURE 4 Stoniness percentage in L and D plots along the soil profile (left). Root density distribution in L and D plots along the soil profile. Error bars are included, but since their values are low, they are often obscured by the symbols



plots (Table 2). No significant differences were observed between the L and D plots in stand (tree density and age) and geo-physical characteristics (elevation, slope and aspect). Although thinning and management strategies were uniform across the forest, using the actual variation in stand density (tree/ha) among the study plots allowed us to examine the possible effects of density on tree size. DBH decreased with tree density, as expected, but the DBH–density relation did not significantly differ between L and D plots (Supporting Information Figure S6; $p = 0.173$ for the interaction between density and plot type). The cross-sectional area of coarse roots along the soil profile was 83% larger in L than in D plots (Table 2). Additionally, the root density was significantly higher ($p < 0.05$) in the L plots in the top 40 cm where the main root system was located and also in deeper layers (70–100 cm) (Figure 4b). Mean root density was calculated over the entire profile, and root: shoot index did not differ among plots.

Variability in stoniness among plots was large, yet on average, stoniness was significantly higher in the soil profiles of the L plots than those of the D plots (Table 2). This difference was mainly contributed by differences in the deeper layers (60–120 cm; $p < 0.001$; Figure 4a, Table 2). The surface rock cover area was four times higher in the L than in the D plots ($p = 0.004$), while the mean maximum soil depth measured in the trenches was lower in L plots (marginally significant, $p = 0.053$; Table 2).

3.3 | Simple “Bucket” model simulations

Using the simplified “bucket model,” differences in SWC between the L to D plots were quantified, addressing the effects and feedbacks of the observed stoniness characteristics in each plot type (using 2011 data). The simulated SWC at 10–60 cm, where the main root system is located, of L and D plots differed significantly throughout the entire simulation period (on average, $p < 0.001$), with the D plots drying below the tSWC threshold on 30 May, 155 days before the estimated first rain (1 November), reaching SWC of 13.25% at the end of the dry season (Figure 5). The SWC in the L plots remained above the tSWC threshold for the entire

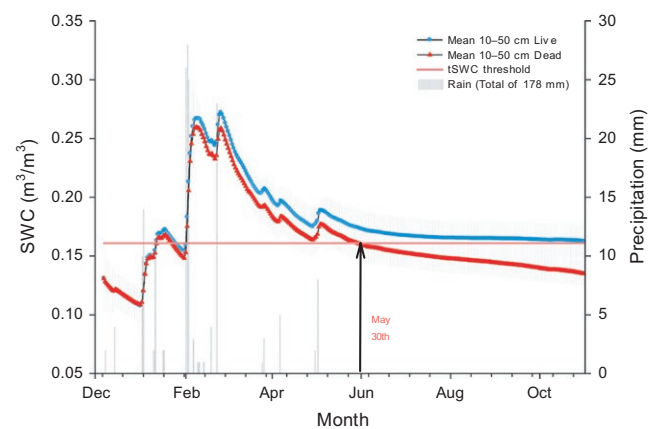


FIGURE 5 Simulated seasonal change in soil moisture (m^3/m^3) in the L and D plots (constrained by observations in the long-term flux site of soil moisture, VPD, ET and rainfall). The observed zero transportable soil water content threshold (tSWC = 0; $0.161 \text{ m}^3/\text{m}^3$) is indicated in orange line. The black arrow indicates the date SWC reached tSWC = 0. The grey area indicates the variations (SD) in simulated SWC across the four depth layers in the 10–50 cm profile. Rainfall data are presented in gray bars, representing values of precipitation as recorded in 2010–2011. ET, evapotranspiration; SWC, soil water content; VPD, vapour pressure deficit

dry season reaching a minimum value of 16.25% at the end of the dry season (Figure 5). The sensitivity analysis (see Supporting Information Table S1, Figure S7) indicated that for SWC levels at the end of the dry season, the dominant factor was the surface rock cover (with a slope of the linear increase in SWC vs. rock cover of ~ 0.1). This was followed by weak negative effect of increasing stone water storage capacity (slope of a linear fit of ~ 0.07) and near-neutral net effect of stoniness in the profile (Figure 6).

4 | DISCUSSION

4.1 | Tree-scale heterogeneity

The results indicated that stress level could be visually identified, which was consistent with the subsequent analysis of specific tree

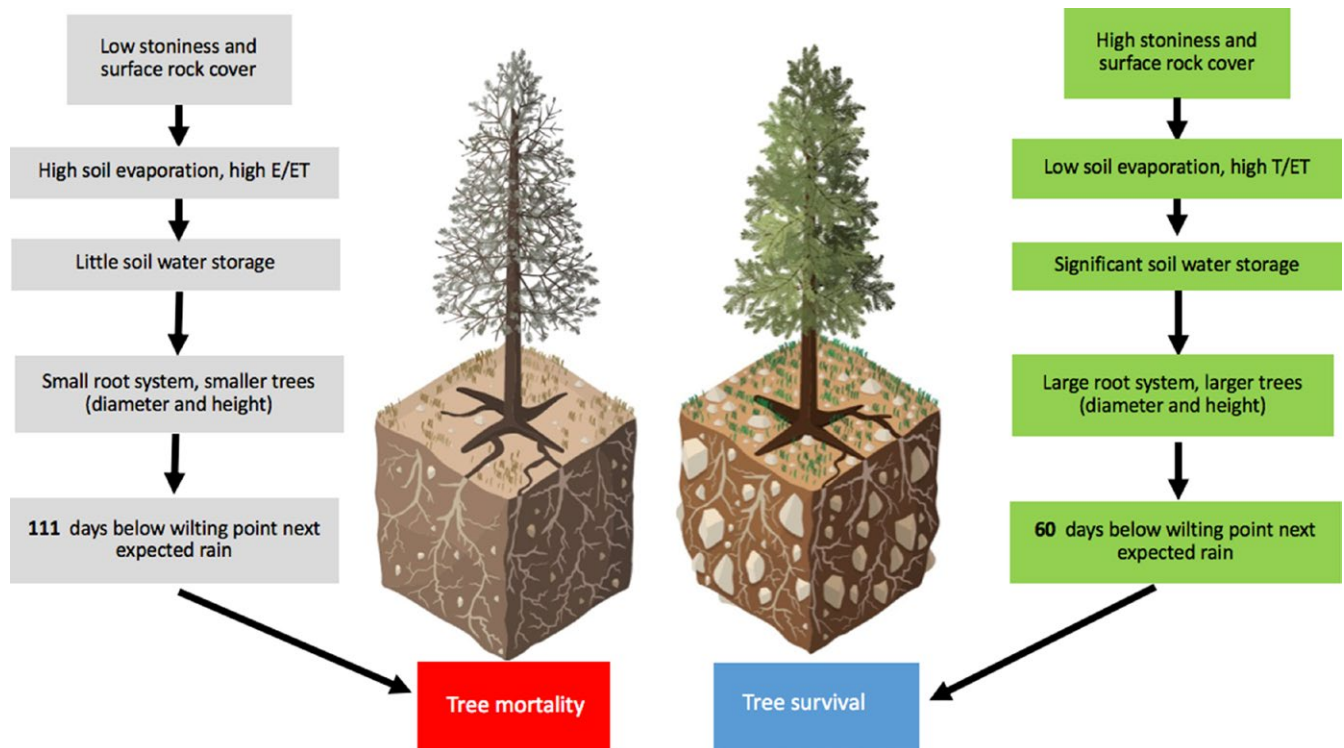


FIGURE 6 A proposed conceptual sequence to mortality or survival associated with observed site variability in stoniness and rock cover, indicating the simulated shortening in of the period with no transpirable soil moisture content in the study site where seasonal drought can last well over 6 months

parameters. This pointed out to a few simple stress indicators that could help in identifying the progress and distribution of drought stress effects across the forest and, in turn, help in optimizing forest management. An effective indicator for tree vulnerability was needle length which decreased relatively fast to drought stress and provided a visible indicator for the stress heterogeneity in the forest as suggested in a previous study (Dobbertin, 2005). Another clear indicator of the stress distribution was a decrease in above-ground biomass, which seemed to also provide an indicator for potential tree mortality. This is consistent with previous studies that showed a higher stress level in smaller trees than in larger ones (Dobbertin, Baltensweiler, & Rigling, 2001). Large biomass also provided the tree with a larger diameter roots (Table 2, Figure 4b), more extensive water conduits, improved tree water storage (Klein et al., 2016) and consequently improved resistance to prolonged dry conditions. The above-ground biomass in the D plots was <60% of the biomass in L plots. Therefore, identifying a specific “biomass” threshold, integrating the tree rings and total DBH, needle length, can provide a useful indicator for tree-scale vulnerability to drought, and management guidance in an evenly aged stand, such as the Yatir Forest.

The most effective vulnerability indicator was the tree rings record, consistent with earlier reports (Cailleret et al., 2017; Camarero, Gazol, Sangüesa-Barreda, Oliva, & Vicente-Serrano, 2015; Mamet, Chun, Metsaranta, Barr, & Johnstone, 2015). Our dendrochronological analysis demonstrated that the “stress-state” of the trees can be identified years prior to mortality, and it is continuously evolving over extended periods, reflected in smaller growth increments in the

stressed versus non-stressed trees. The tree ring analyses revealed two main aspects of the drought effects. First, exposed to the same stressor, trees that were visibly assigned to the three different stress levels in 2011 showed different growth responses to precipitation over time. Second, these differential trends were induced by signature drought events that could lead to mortality up to 25 years later. Both stressed and dying trees developed similarly long-term downward shift in their BAI trend, compared to non-stressed trees, but in stressed trees, divergence started about 10 years later than the most stressed trees that died off in the 2010 event. Notably, the intermediately stressed trees did not recover following signature wet years (e.g., 1991–1992, or 2001–2003).

We hypothesize that these differential response patterns reflect a combination of two effects. First, a permanent difference was generated in trees during the signature years, for example in root distribution and density, due to a low volumetric water content in soils of low stoniness (see below). This was reflected in the increasing differences in tree size as indicated by cumulative BAI. Second, permanent differences in soil moisture conditions at the scale of the individual tree could underlie the difference in summer pre-dawn WP. Such effects could be expected to increase with time as tree size and water demands increase or as a consequent result limited crown and root size. In both cases, the effects that were reflected in the onset of the differential tree ring patterns would lead to a cascade of stress effects and eventually to the observed mortality (Anderegg et al., 2013; Bert, 1993; McDowell, 2011; Peltier et al., 2016).

4.2 | Plot-scale heterogeneity

The most striking observations made in this study are the highly distinct plot-scale heterogeneity in mortality. This was first noted in aerial photography reported by the forestry services (not shown), which led to our ground-level investigation. In spite of the low mean annual precipitation and the severe drought years preceding this study (Figure 3), there were large patches of forest with little mortality (<20%; L plots), while full-blown mortality (>80%; D plots) was observed in other forest plots. A careful check of a wide range of parameters indicates that these plot-scale differences could not be explained by differences stand density, tree age, soil type, slope or aspect, which were insignificant (Table 2). The only clear difference between plots we could identify was in stoniness and surface rock cover (Table 2, Figure 4).

Shallow but large-surface rocks at or near the soil surface can have two effects. First, it creates a local run-off concentrating the rainfall on a given patch of soil into a reduced area, likely increasing the rate of water percolation into the soil. Second, it protects the soil beneath it from evaporation. The “concentrating” effect involves some trade-offs and is likely the minor effect: Increasing the moisture “concentration” in the stone-free soil can extend the time during the dry season when SWC is above the wilting point. But higher SWC also enhances evaporation from the stone-free soil surface. In contrast, the “mulching effect” of partially covering the soil surface does not involve this trade-off and (assuming near-zero evaporation from the rock surface) can be expected to be in direct proportion to the increase in this parameter in the L plots.

Increased stoniness across the soil profile could also help explain the L versus D plot differences. First, the higher stone content may suggest that fractured bedrock is within reach of the tree roots, and these fractures could hold water reachable by the root system. This hypothesis, while valid in other regions (e.g., Kukowski, Schwinning, & Schwartz, 2013; Nardini et al., 2016), is unlikely to be so at our study site. Our trenching in the L plots penetrated into the bedrock (see Supporting Information Appendix S1) showing no visibly increased fractures and no root presence (see also Figure 4 and Supporting Information Figure S2). Note also that previous studies at our site indicated a sharp increase in clay content with depth in the shallow soil, resulting in high soil water retention, and helped explain the shallow root system and tree survival during low precipitation periods. Finally, we also note that Aleppo pine trees (in general and in our site specifically) have a shallow flat root system, without a main tap root penetrating to depth, such as observed in other species.

Second, stoniness in the soil profile reduces the stone-free soil volume and while it decreases its absolute soil water capacity, it also increases its “concentration” (m^3/m^3). Note that this is particularly so for the study site, previously characterized with no significant run-off, drainage, lateral flow or recharge to depth (Klein, Hoch, Yakir, & Körner, 2014; Yaseef et al., 2009). Due to the nonlinear relationship between SWC and soil WP, a small increase in SWC can lead

to a large increase in soil WP, which in turn can result in more accessible water for root uptake. Here too, this effect involves some trade-offs. Increased SWC also increases soil evaporation, but this effect may decrease with depth and help maintain in the lower soil layers the SWC above the wilting point for longer periods in the long dry season. Furthermore, the significantly larger trees in the L plots (Table 2) are associated with higher transpiration rate, mainly in the wet season, and higher SWC at the lower soil layers could help support this enhanced flux (and the associated productivity) and further minimize the loss to soil surface evaporation, and ultimately leading to reduced mortality. Finally, as the chalky stones can store water and release it under dry conditions, increased stoniness also enhances this storage capacity, which can become critical in the long dry season (up to 11 months without significant amounts of rain, as observed in 2008–2009). Trade-offs, in this case, can be associated with the initial removal of water from the soil into the stone, reducing SWC of the stone-free soil. This is compensated for by the slow release of water when the soil dries and the stone–soil water concentration gradient is reversed.

Our observations are consistent with the potential effects of increased surface rock cover and stoniness discussed above, and provide the only hypothesis we can offer at present to explain the plot-scale heterogeneity in mortality. However, our measurements are not sufficient at this stage to validate our hypothesis and account for all the effects and feedbacks discussed above. A preliminary attempt to corroborate our empirical results from an ecosystem perspective was made using a simple bucket model. While our model does not include the full complexity of the system, it was strongly constrained by the wealth of long-term observations at our flux site, of precipitation (P), ET, sap flow (SF), SWC dynamics and meteorology. It provided a clear indication that the combined effects of surface rock cover and stoniness are a plausible hypothesis to help explain the striking plot-scale heterogeneity in mortality we observed (Figure 5). These results indicated that in the D plots, SWC can reach the wilting point and strongly limit transpiration in early summer (May 30th), while in the L plots, SWC could remain above the wilting point essentially until the next rainy season that usually starts in November. The sensitivity analysis for the three main parameters (surface rock cover, stoniness in the soil profile and stone water storage capacity) indicated that the surface rock cover has the strongest, and near linear, effect (Supporting Information Table S1). This is likely due predominantly to the protection of SWC from surface evaporation. The weaker and apparent negative response of SWC to variations in stone water storage capacity reflects the fact that increasing stone water storage removes water from the stone-free soil, but this effect is compensated for by the slow release of water during the dry season when the soil–stone gradient is reversed and some of this water is expected to return to the stone-free soil in the most stressful period. Notably, the near-neutral response of SWC at the end of the dry season to variations in stoniness in the soil profile (Supporting Information Table S1) seems to reflect a “net” effect, preventing the overdrying of the soil in the L plots

while supporting tree transpiration 15% higher during the wet period than in the D plots.

More research into the role of surface rock cover and stoniness in the survival of trees in the face of increasing droughts is needed. Note in that respect that our findings are different than some previous results in very different environments (e.g., in northern Patagonia with ~3,000 mm rainfall; Suarez et al., 2004) that indicated that rocky and shallow soils sites are vulnerable to drought-related tree mortality. In dry environments, our results are consistent with earlier studies (e.g., Kadmon, Yair, & Danin, 1989) that reported a positive effect of rock fragments on the abundance of woody perennials and attributed it to the favourable effects on water availability, and with other cases reviewed by Poesen and Lavee (1994). To our knowledge, however, this is the first study that provides quantitative evidence to the proposed relationship between increased rock fragments and stoniness and tree reduced mortality in water-limited areas.

Finally, our tentative modelling results support our working hypothesis that with the lack of any other clear driver, the increase in the extent of surface rock cover and soil stoniness provides a feasible mechanism to reduce mortality in harsh conditions such as in the Yatir Forest. This, in turn, can help explain the unusual spatial patterns of tree survival in the study site and could assist forest management and modelling of forest ecosystems in dry conditions.

ACKNOWLEDGEMENTS

This long-term study was funded by KKL (project number: 90-10-012-11), the German Research Foundation (DFG) as part of the project "Climate feedbacks and benefits of semi-arid forests" (Cliff), by a grant from the Ministry of Science & Technology, Israel, and by the Ministry of Foreign Affairs and International Development (MAEDI) and the Ministry of National Education, Higher Education and Research (MENESR) of France (IMOS-French Program: 3-6735). The authors want to thank Efrat Schwartz for assistance with laboratory work and Noam Weisbrod for fruitful discussions and help with the manuscript.

AUTHORS' CONTRIBUTIONS

Y.P., E.R., I.M., J.M.G. and D.Y. conceived the ideas and designed methodology; Y.P., D.B., S.R., N.H. and T.K. collected the data. Y.P., F.T., J.M.G., J.O., L.W., N.H. and D.B. analysed the data. Y.P., J.M.G., F.T. and D.Y. led the writing of the manuscript. All authors contributed critically to the drafts and gave final approval for publication.

DATA ACCESSIBILITY

Data upon which this study is based are available through the Dryad Digital Repository <https://doi.org/10.5061/dryad.92dj50c> (Preisler et al., 2019).

ORCID

Yakir Preisler  <https://orcid.org/0000-0001-5861-8362>

Tamir Klein  <https://orcid.org/0000-0002-3882-8845>

REFERENCES

- Allen, C. D., Macalady, A. K., Chenchouni, H., Bachelet, D., McDowell, N., Vennetier, M., ... Cobb, N. (2010). A global overview of drought and heat-induced tree mortality reveals emerging climate change risks for forests. *Forest Ecology and Management*, 259(4), 660–684. <https://doi.org/10.1016/j.foreco.2009.09.001>
- Alpert, P., Krichak, S. O., Shafir, H., Haim, D., & Osetinsky, I. (2008). Climatic trends to extremes employing regional modeling and statistical interpretation over the E. Mediterranean. *Global and Planetary Change*, 63(2–3), 163–170. <https://doi.org/10.1016/J.GLOPLACHA.2008.03.003>
- Anderegg, W. R. L., Berry, J. A., Smith, D. D., Sperry, J. S., Anderegg, L. D. L., & Field, C. B. (2012). The roles of hydraulic and carbon stress in a widespread climate-induced forest die-off. *Proceedings of the National Academy of Sciences of the United States of America*, 109(1), 233–237. <https://doi.org/10.1073/pnas.1107891109>
- Anderegg, W. R. L., Plavcová, L., Anderegg, L. D. L., Hacke, U. G., Berry, J. A., & Field, C. B. (2013). Drought's legacy: Multiyear hydraulic deterioration underlies widespread aspen forest die-off and portends increased future risk. *Global Change Biology*, 19(4), 1188–1196. <https://doi.org/10.1111/gcb.12100>
- Bert, G. D. (1993). Impact of ecological factors, climatic stresses, and pollution on growth and health of silver fir (*Abies alba* Mill.) in the Jura mountains: An ecological and dendrochronological study. *Acta Oecologica*, 14(2), 229–246.
- Breshears, D. D., Myers, O. B., Meyer, C. W., Barnes, F. J., Zou, C. B., Allen, C. D., ... Pockman, W. T. (2009). Tree die-off in response to global change-type drought: Mortality insights from a decade of plant water potential measurements. *Frontiers in Ecology and the Environment*, 7(4), 185–189. <https://doi.org/10.1890/080016>
- Cailleret, M., Jansen, S., Robert, E. M. R., Desoto, L., Aakala, T., Antos, J. A., ... Martínez-Vilalta, J. (2017). A synthesis of radial growth patterns preceding tree mortality. *Global Change Biology*, 23(4), 1675–1690. <https://doi.org/10.1111/gcb.13535>
- Camarero, J. J., Gazol, A., Sangüesa-Barreda, G., Oliva, J., & Vicente-Serrano, S. M. (2015). To die or not to die: Early warnings of tree dieback in response to a severe drought. *Journal of Ecology*, 103(1), 44–57. <https://doi.org/10.1111/1365-2745.12295>
- Colangelo, M., Camarero, J. J., Borghetti, M., Gazol, A., Gentilesca, T., & Ripullone, F. (2017). Size matters a lot: Drought-affected Italian oaks are smaller and show lower growth prior to tree death. *Frontiers in Plant Science*, 8(February), 1–14. <https://doi.org/10.3389/fpls.2017.00135>
- Dickman, L. T., McDowell, N. G., Sevanto, S., Pangle, R. E., & Pockman, W. T. (2015). Carbohydrate dynamics and mortality in a piñon-juniper woodland under three future precipitation scenarios. *Plant, Cell & Environment*, 38, 729–739. <https://doi.org/10.1111/pce.12441>
- Dobbertin, M. (2005). Tree growth as indicator of tree vitality and of tree reaction to environmental stress: A review. *European Journal of Forest Research*, 124(4), 319–333. <https://doi.org/10.1007/s10342-005-0085-3>
- Dobbertin, M., Baltensweiler, A., & Rigling, D. (2001). Tree mortality in an unmanaged mountain pine (*Pinus mugo* var. *uncinata*) stand in the Swiss National Park impacted by root rot fungi. *Forest Ecology and Management*, 145(1–2), 79–89. [https://doi.org/10.1016/S0378-1127\(00\)00576-4](https://doi.org/10.1016/S0378-1127(00)00576-4)
- Dorman, M., Perevolotsky, A., Sarris, D., & Svoray, T. (2015). Amount vs. temporal pattern: On the importance of intra-annual

- climatic conditions on tree growth in a dry environment. *Journal of Arid Environments*, 118, 65–68. <https://doi.org/10.1016/j.jaridenv.2015.03.002>
- Eckstein, D., & Bauch, J. (1969). Beitrag zur Rationalisierung eines dendrochronologischen Verfahrens und zur Analyse seiner Aussagesicherheit. *Forstwissenschaftliches Centralblatt*, 88(1), 230–250. <https://doi.org/10.1007/BF02741777>
- Gao, X., & Giorgi, F. (2008). Increased aridity in the Mediterranean region under greenhouse gas forcing estimated from high resolution simulations with a regional climate model. *Global and Planetary Change*, 62(3–4), 195–209. <https://doi.org/10.1016/j.gloplacha.2008.02.002>
- Gitlin, A. R., Sthultz, C. M., Bowker, M. A., Stumpf, S., Paxton, K. I., Kennedy, K., ... Whitham, T. G. (2006). Mortality gradients within and among dominant plant populations as barometers of ecosystem change during extreme drought. *Conservation Biology*, 20(5), 1477–1486. <https://doi.org/10.1111/j.1523-1739.2006.00424.x>
- Grünzweig, J. M., Gelfand, I., Fried, Y., & Yakir, D. (2007). Biogeochemical factors contributing to enhanced carbon storage following afforestation of a semi-arid shrubland. *Biogeosciences*, 4(5), 891–904. <https://doi.org/10.5194/bg-4-891-2007>
- Hlaváčiková, H., Novák, V., & Šimůnek, J. (2016). The effects of rock fragment shapes and positions on modeled hydraulic conductivities of stony soils. *Geoderma*, 281, 39–48. <https://doi.org/10.1016/j.geoderma.2016.06.034>
- Huang, C.-Y., & Anderegg, W. R. L. (2012). Large drought-induced aboveground live biomass losses in southern Rocky Mountain aspen forests. *Global Change Biology*, 18(3), 1016–1027. <https://doi.org/10.1111/j.1365-2486.2011.02592.x>
- IPCC (Intergovernmental Panel on Climate Change). (2013). *Climate change 2013*. T. Stocker et al. (Eds.), Cambridge, UK: Cambridge University Press.
- Kadmon, R., Yair, A., & Danin, A. (1989). Relationship between soil properties, soil moisture, and vegetation along loess-covered hillslopes, northern Negev, Israel. *Catena Supplement*, 14, 43–57.
- Klein, T., Cohen, S., Paudel, I., Preisler, Y., Rotenberg, E., & Yakir, D. (2016). Diurnal dynamics of water transport, storage and hydraulic conductivity in pine trees under seasonal drought. *iForest*, 9(5), 710–719. <https://doi.org/10.3832/for2046-009>
- Klein, T., Cohen, S., & Yakir, D. (2011). Hydraulic adjustments underlying drought resistance of *Pinus halepensis*. *Tree Physiology*, 31(6), 637–648. <https://doi.org/10.1093/treephys/tpq047>
- Klein, T., Hoch, G., Yakir, D., & Körner, C. (2014). Drought stress, growth and nonstructural carbohydrate dynamics of pine trees in a semi-arid forest. *Tree Physiology*, 34(9), 981–992. <https://doi.org/10.1093/treephys/tpu071>
- Klein, T., Rotenberg, E., Cohen-Hilaleh, E., Raz-Yaseef, N., Tatarinov, F., Preisler, Y., ... Yakir, D. (2012). Quantifying transpirable soil water and its relations to tree water use dynamics in a water-limited pine forest. *Ecohydrology*, 7(2), 409–419. <https://doi.org/10.1002/eco.1360>
- Koepke, D. F., Kolb, T. E., & Adams, H. D. (2010). Variation in woody plant mortality and dieback from severe drought among soils, plant groups, and species within a northern Arizona ecotone. *Oecologia*, 163(4), 1079–1090. <https://doi.org/10.1007/s00442-010-1671-8>
- Kukowski, K. R., Schwinning, S., & Schwartz, B. F. (2013). Hydraulic responses to extreme drought conditions in three co-dominant tree species in shallow soil over bedrock. *Oecologia*, 171, 819–830. <https://doi.org/10.1007/s00442-012-2466-x>
- Mamet, S. D., Chun, K. P., Metsaranta, J. M., Barr, A. G., & Johnstone, J. F. (2015). Tree rings provide early warning signals of jack pine mortality across a moisture gradient in the southern boreal forest. *Environmental Research Letters*, 10(8), 84021. <https://doi.org/10.1088/1748-9326/10/8/084021>
- Maseyk, K. S., Lin, T., Rotenberg, E., Grünzweig, J. M., Schwartz, A., & Yakir, D. (2008). Physiology-phenology interactions in a productive semi-arid pine forest. *The New Phytologist*, 178(3), 603–616. <https://doi.org/10.1111/j.1469-8137.2008.02391.x>
- McDowell, N. G. (2011). Mechanisms linking drought, hydraulics, carbon metabolism, and vegetation mortality. *Plant Physiology*, 155(3), 1051–1059. <https://doi.org/10.1104/pp.110.170704>
- McDowell, N., Pockman, W. T., Allen, C. D., Breshears, D. D., Cobb, N., Kolb, T., ... Yepez, E. A. (2008). Mechanisms of plant survival and mortality during drought: Why do some plants survive while others succumb to drought? *The New Phytologist*, 178(4), 719–739. <https://doi.org/10.1111/j.1469-8137.2008.02436.x>
- Nardini, A., Casolo, V., Borgo, A. D., Savi, T., Stenni, B., Bertoncin, P., ... Mestre, V. (2016). Rooting depth, water relations and non-structural carbohydrate dynamics in three woody angiosperms differentially affected by an extreme summer drought. *Plant, Cell & Environment*, 39(3), 618–627. <https://doi.org/10.1111/pce.12646>
- Novák, V., Kňava, K., & Šimůnek, J. (2011). Determining the influence of stones on hydraulic conductivity of saturated soils using numerical method. *Geoderma*, 161(3–4), 177–181. <https://doi.org/10.1016/j.geoderma.2010.12.016>
- Oppenheimer, H. R. (1957). The influence of the soil on the development and the mineral composition of the Aleppo pine. *La Yaaran*, 7(3/4), 5–9.
- Padilla, F. M., Miranda, J. D., & Pugnaire, F. I. (2007). Early root growth plasticity in seedlings of three Mediterranean woody species. *Plant and Soil*, 296(1), 103–113. <https://doi.org/10.1007/s11104-007-9294-5>
- Parolari, A. J., Katul, G. G., & Porporato, A. (2014). An ecohydrological perspective on drought-induced forest mortality. *Journal of Geophysical Research: Biogeosciences*, 119, 965–981. <https://doi.org/10.1002/2013JG002592>
- Peltier, D. M. P., Fell, M., & Ogle, K. (2016). Legacy effects of drought in the southwestern United States: A multi-species synthesis. *Ecological Monographs*, 86(3), 312–326. <https://doi.org/10.1002/ecm.1219>
- Peterman, W., Waring, R. H., Seager, T., & Pollock, W. L. (2013). Soil properties affect pinyon pine—Juniper response to drought. *Ecohydrology*, 6(3), 455–463. <https://doi.org/10.1002/eco.1284>
- Poesen, J., & Lavee, H. (1994). Rock fragments in top soils: significance and processes. *Catena*, 23, 1–28.
- Porra, R. J. (2002). The chequered history of the development and use of simultaneous equations for the accurate determination of chlorophylls a and b. *Photosynthesis Research*, 73(1–3), 149–156. <https://doi.org/10.1023/A:1020470224740>
- Preisler, Y., Tatarinov, F., Grünzweig, J. M., Bert, D., Ogée, J., Wingate, L., ... Yakir, D. (2019). Data from: Mortality versus survival in drought-affected Aleppo pine forest depends on the extent of rock cover and soil stoniness. *Dryad Digital Repository*, <https://doi.org/10.5061/dryad.92dj50c>
- Ritchie, J. T. (1981). Soil water availability. *Plant and Soil*, 58(1), 327–338.
- Schiller, G., & Atzmon, N. (2009). Performance of Aleppo pine (*Pinus halepensis*) provenances grown at the edge of the Negev desert: A review. *Journal of Arid Environments*, 73(12), 1051–1057. <https://doi.org/10.1016/j.jaridenv.2009.06.003>
- Schweingruber, F. H., Bartholin, T., Schaur, E., & Briffa, K. R. (1988). Radiodensitometric-dendroclimatological conifer chronologies from Lapland (Scandinavia) and the Alps (Switzerland). *Boreas*, 17(4), 559–566. <https://doi.org/10.1111/j.1502-3885.1988.tb00569.x>
- Slayter, R. O. (1967). *Plant-water relationships*. Plant-Water Relationships. London, New York, NY: Academic Press. Retrieved from <https://www.cabdirect.org/cabdirect/abstract/19680700504>
- Soulé, P. T., & Knapp, P. A. (2007). Topoedaphic and morphological complexity of foliar damage and mortality within western juniper (*Juniperus occidentalis* var. *occidentalis*) woodlands following an extreme meteorological event. *Journal of Biogeography*, 34(11), 1927–1937. <https://doi.org/10.1111/j.1365-2699.2007.01743.x>

- Suarez, M. L., Ghermandi, L., & Kitzberger, T. (2004). Factors predisposing episodic drought-induced tree mortality in *Nothofagus*-site, climatic sensitivity and growth trends. *Journal of Ecology*, 92(6), 954–966.
- Tatarinov, F., Rotenberg, E., Maseyk, K., Ogée, J., Klein, T., & Yakir, D. (2016). Resilience to seasonal heat wave episodes in a Mediterranean pine forest. *New Phytologist*, 210(2), 485–496.
- Worrall, J. J., Egeland, L., Eager, T., Mask, R. A., Johnson, E. W., Kemp, P. A., & Shepperd, W. D. (2008). Rapid mortality of *Populus tremuloides* in southwestern Colorado, USA. *Forest Ecology and Management*, 255(3–4), 686–696. <https://doi.org/10.1016/j.foreco.2007.09.071>
- Yaseef, N. R., Yakir, D., Rotenberg, E., Schiller, G., & Cohen, S. (2009). Ecohydrology of a semi-arid forest: Partitioning among water balance components and its implications for predicted precipitation changes. *Ecohydrology*, 3, 143–154. <https://doi.org/10.1002/eco>

SUPPORTING INFORMATION

Additional supporting information may be found online in the Supporting Information section at the end of the article.

How to cite this article: Preisler Y, Tatarinov F, Grünzweig JM, et al. Mortality versus survival in drought-affected Aleppo pine forest depends on the extent of rock cover and soil stoniness. *Funct Ecol*. 2019;00:1–12. <https://doi.org/10.1111/1365-2435.13302>